IEEE Open Journal of
Antennas and Propagation

Received 4 October 2023; revised 5 December 2023; accepted 10 December 2023. Date of publication 14 December 2023; date of current version 30 January 2024.

Digital Object Identifier 10.1109/OJAP.2023.3342934

Low-SAR and High-FBR Patch Antenna With Small Ground Size for Wearable Devices

SHU-WEI YU [1] (Student Member, IEEE), XIAO ZHANG [1] (Member, IEEE), QIONG-SEN WU [2] (Member, IEEE), LEI ZHU [3] (Fellow, IEEE), TAO YUAN [1] (Member, IEEE), AND QING-HUA JIANG [4]

[1]College of Information Engineering, Shenzhen University, Shenzhen 518060, China

[2]School of Integrated Circuits, Guangdong University of Technology, Guangzhou 510006, China

[3]Faculty of Science and Technology, University of Macau, Macau, China

[4]Devision of Watch Phone, Guangdong Little Genius Technology Ltd., Dongguan 523000, China

CORRESPONDING AUTHORS: X. ZHANG AND Q.-H. JIANG (e-mail: xiao.zhang@szu.edu.cn; jiangqh@eebbk.com)

This work was supported in part by the National Key Research and Development Program, China, under Project 2023YFB4403800; in part by the Guangdong Provincial Department of Science and Technology, China, under Project 2020B1212030002; in part by the Shenzhen Science and Technology Innovation Commission, China, through the Construction and Operation Project of Guangdong Provincial Key Laboratory and Guangdong–Hong Kong–Macau Joint Laboratory under Project CJGJZD2022051714240411 and Project KQTD20180412181337494; in part by the Postgraduate Education Branch of the China Education Society of Electronics; and in part by the Guangdong Provincial Department of Education, China, through the Innovation Team Project under Grant 2020KCXTD004.

ABSTRACT A high front-to-back ratio (FBR) microstrip patch antenna with small ground plane size is proposed and studied in this article. In order to suppress the serious back lobe brought by such a small ground, a hybrid loading technique consisting of coupled branch (CB) and resistor-loaded ground slot (RLGS) is introduced. Through the hybrid loading, extra magnetic currents on the ground are excited, by which the backward radiation of the original patch could be cancelled. In addition, the joint regulation mechanism of CB and RLGS is expressed as an equivalent circuit model, which provides more physical insight. The realized FBR of the proposed antenna reaches over 38 dB, as a result, the specific absorption rate (SAR) of the antenna under wearable conditions is suppressed, and the radiation efficiency is nearly unaffected by the human body, which is highly demanded by wearable devices.

INDEX TERMS Front-to-back ratio, microstrip patch antenna, resistor-loading technique, specific absorption rate.

I. INTRODUCTION

IN THE tide of intelligent terminal development, the miniaturization of the antenna size is constantly emphasized. However, the ground plane size has been largely excluded from the discussion of miniaturizing microstrip antennas. As a matter of fact, when it comes to the real applications in portable/wearable devices, the size reduction of the ground plane in an antenna becomes a vital issue.

Nevertheless, it is widely recognized that the overall size of a ground plane has a tremendous impact on the far-zone radiation performance of a microstrip antenna [1], [2], [3]. So far, many researches in theory and practice have been conducted on the correlation between the finite ground size and the front-to-back ratio (FBR) of patch antennas [4], [5]. Several studies have revealed the fact that with the shrink of the ground screen, the back lobe level of a patch antenna magnifies as a whole. In fact, remarkable backward radiation is not a positive virtue for any directional antenna. It produces harmful interferences to other circuits behind the antenna. What is more, when used in wearable devices, long-time exposure of human organism under backward radiation from the antenna might cause prospective health risks. The body absorption rate of the radiation is commonly evaluated by the specific absorption rate (SAR) [6], [7], [8], and the SAR problem has become a huge challenge for the antenna design of wearable devices. Thus, it is necessary to suppress

the backward radiation of an antenna while preserving a comparatively finite ground plane size.

Yagi-Uda-like antenna is one of the most representative directive antennas [9], [10], [11]. However, its end-fire radiation is not capable for wearable devices. Cavities and reflectors are also employed for FBR enhancement, especially in base stations [12], [13], [14], [15]. But their overall profiles are significantly larger than patch antennas, in which there is a trade-off.

Serrated/Curved ground edge is a technique which reduces ground edge current intensity and suppresses the nearby diffracted waves [16], [17], [18]. However, the backward radiation lessening effect decreases as the ground plane size shrinks.

The magneto-electric (ME) dipole technique is also effective for enhanced FBR, in which complementary magnetic source and electric source are constructed with specific antenna structure [19], [20]. Despite this technic cannot be directly applied to microstrip antenna, its mechanism is inspiring.

Besides, slot loading is a distinctive method with similar principle. The loaded slots introduce extra induced magnetic currents in order to cancel the edge wave diffraction [21], [22], [23]. Another unique method is to introduce a slotted parasitic conductor disc under electrically small antenna to achieve high FBR [24]. This technique declines the backward radiation effectively. In the meantime, its theoretical analysis remains huge potential for improvement. What is more, under the circumstances that the antenna ground plane size is strictly limited, the difficulty of FBR increasement will rise.

In this article, a novel FBR enhancing method, which simultaneously adopts coupled branch (CB) and resistor-loaded ground slot (RLGS) technique, is applied to a patch antenna. Through creating extra controllable magnetic currents on the ground, the FBR of the proposed patch is greatly increased, and the ground size remains a very small size. In particular, the SAR of the proposed antenna under the wearable condition is dramatically eliminated due to the FBR development.

II. ANTENNA CONFIGURATION AND ANALYSIS

In this section, a novel microstrip antenna structure with small ground size and near-zero backward radiation is proposed and discussed, and its working principle and equivalent circuit model are rigorously analyzed as follows.

In order to facilitate the lightweight, cheap, and small-size advantages of portable devices, FR-4 substrate with height of 1.2 mm and relative permittivity of 4.4 is employed. The distance *DA* and *DB* from the ground edge to the patch are respectively 0.06 λ_0 and 0.02 λ_0, which implies that the ground plane size of the proposed patch is comparatively small. The detailed size data are listed in Table 1.

In Fig. 1(a) there are four rectangular coupled branches extended from the radiating edges of the patch, whose opposite ends are connected to the grounded via holes.

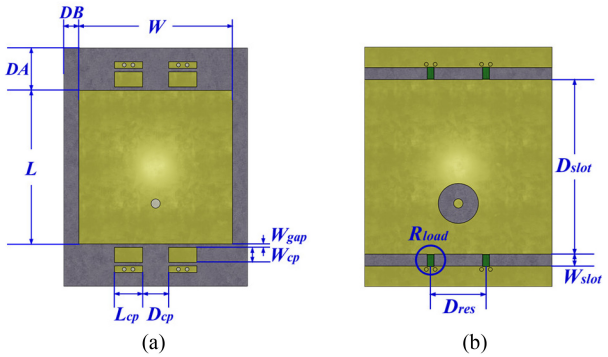

FIGURE 1. (a) Top view (b) Bottom view of the proposed microstrip antenna.

TABLE 1. Parameters of the proposed antenna.

Parameter	W	L	DA	DB	W_{gap}	D_{cp}
Value (mm)	11.6	11.7	3.15	1.20	0.26	1.98
Parameter	W_{cp}	L_{cp}	D_{slot}	W_{slot}	D_{res}	R_{load}
Value (mm)	1.13	2.14	13.08	0.89	4.12	82Ω

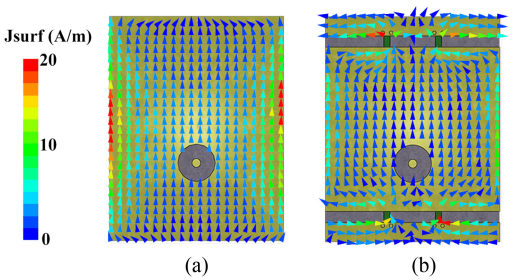

FIGURE 2. The surface current distribution on the back side of the ground (a) without RLGS loading and (b) with RLGS loading.

The bottom layer structure is shown in Fig. 1(b), on which there are two parallel slots constructed. Four lumped resistors (R_{load}) symmetrically bridge over the ground slot structures, which constitutes a circuit loop with the CB through the vias.

The fundamental working principle is explained as follows. Firstly, as illustrated in Fig. 2, due to the absorbing effect of the lumped resistors, the surface current on the back of the ground slightly diminishes after RLGS is loaded, which contributes to the suppression of backlobe.

However, it is unrealistic to eliminate the back surface current by loading resistors merely, especially when the ground size is sorely limited. Thus the CB structure is introduced in order to counterbalance backward radiation. The working mechanism of the CB structure is shown in Fig. 3(a). Due to the coupling capacitance between the patch and CB, extra current routes arise. As a result, an artificial magnetic current I_s^m controlled by the CB currents is established. As is demonstrated in Fig. 3(b), the tangential electric fields at the radiating edge of the patch and those at the ground slot can be equivalent as a pair of oppositely-oriented magnetic currents.

The sketch of the far-field pattern superposition of the magnetic currents is illustrated in Fig. 4. Due to the finite

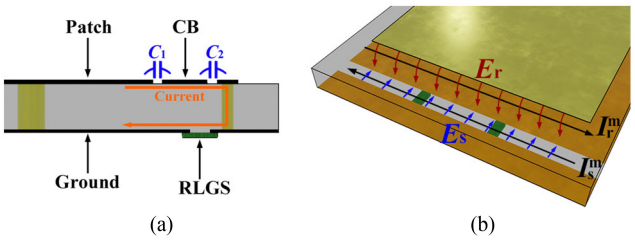

FIGURE 3. (a) The current route flowing through the CB and RLGS structure from the side view. (b) A pair of oppositely-directed magnetic sources triggered by the current loop. (The CB structure is hidden in order to make the figure clear.)

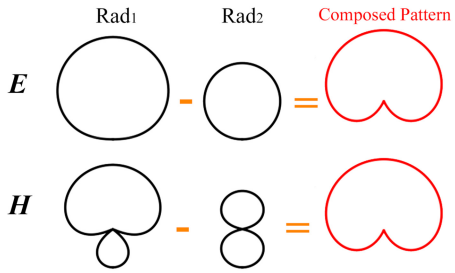

FIGURE 4. The superposition of the E/H-plane far-field patterns (Rad_1 and Rad_2) of the oppositely-directed magnetic currents.

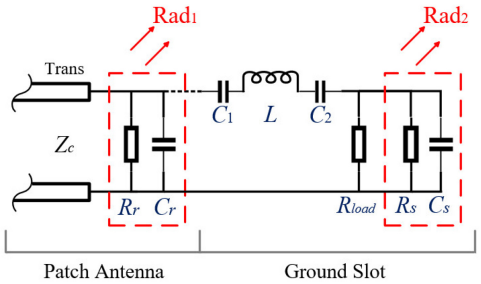

FIGURE 5. The equivalent circuit model of the CB and RLGS structure.

ground effect, the radiation pattern of the original patch (Rad_1) has a high backward lobe level, which is neutralized by the far fields of the magnetic current (Rad_2) in the ground slots. The Rad_2 far-field is bidirectional and phase-inverted, once the intensity of the ground slot source is properly adjusted, the backward radiation can be theoretically eliminated.

The equivalent circuit model is presented in Fig. 5. In this model, the radiating edge of the patch is perceived as a parallel circuit of radiation resistance (R_r) and capacitance (C_r), and the ground slot is perceived as parallel R_s and C_s. The RLGS resistors bridged over the ground slot are denoted as R_{load}. The tightly coupled CB structure is modeled as a series of coupling capacitance (C_1, C_2) and the parasitic inductance (L) of the CB conductor. The voltage V_r across the resistor R_r is considered as constant. Thus the voltage V_s across the R_s can be expressed as:

$$\frac{V_s}{V_r} = \left[\left(\frac{1}{j\omega C_1} + \frac{1}{j\omega C_2} + j\omega L\right)\left(\frac{1}{R_{load}} + \frac{1}{R_s} + j\omega C_s\right) + 1\right]^{-1} \quad (1)$$

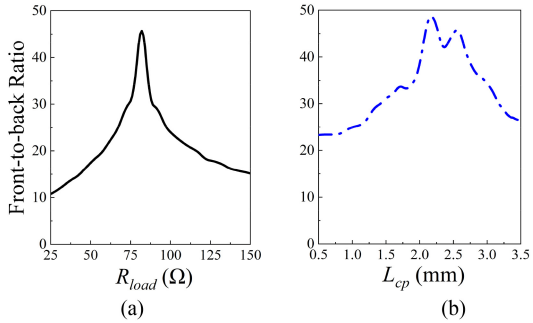

FIGURE 6. The simulated FBR curves of the proposed patch antenna at 5.8GHz as the parameter (a) R_{load} and (b) L_{cp} changes.

According to the expression, the coupling capacitance (C_1, C_2) and the RLGS resistance R_{load} jointly control the phase and magnitude of the voltage V_s across resistor R_s. Further, the radiated power of the ground slot can be adjusted through altering the CB and RLGS structure. It is also worth mentioning that for the purpose of phase control, capacitance C_1 and C_2 are both necessary. If the back lobe levels of Rad_1 and Rad_2 cancel out with each other, the FBR will be significantly developed. It can be deduced that the optimal C_1, C_2, and R_s values correspond to a specific extremum point in the FBR curve. Once those values deviate from the extremum point, the FBR of the proposed antenna will decline as a response.

III. SIMULATION AND MEASUREMENT

A. ANALYSIS OF THE RLGS AND CB STRUCTURES

In order to validate the controllable mechanism of RLGS and CB structure, the proposed model in Fig. 1 is simulated and analyzed in the ANSYS HFSS simulator based on 3-D Finite Element Method (FEM).

In order to discover the loading effect of the RLGS structure, its R_{load} parameter is swept while the CB is fixed to a static state. From Fig. 6(a) it can be seen that the simulated FBR reaches the peak value of 45 dB as R_{load} gradually approaches 82 Ω. And the FBR sharply descends as the R_{load} deviates from this value.

Similarly, if the coupling capacitance C_1 and C_2 in CB is swept while the R_{load} in RLGS is fixed, an analogous phenomenon will happen. The length L_{cp} of CB is altered so as to adjust the coupling capacitance. The result in Fig. 6(b) illustrates a tendency similar to the one in Fig. 6(a), which shows good agreement with the circuit model analysis. This phenomenon can be explained by equation (1), in which the R_{load} and C_1/ C_2 determine the radiated power of the ground slot, and the backward radiation disappears as the power reaches the cancellation point. What is more, the curve in Fig. 6(b) slightly fluctuates, since the CB structure consists of complicated parasitic parameters, which is not as ideal as prescribed.

What is more important, as a result of back lobe reduction, SAR of the proposed patch antenna can be dramatically decreased. As is shown in Fig. 7, the antenna is placed

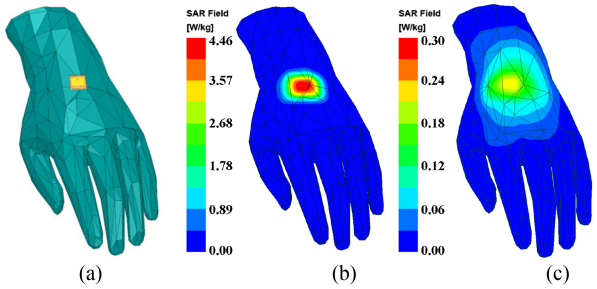

FIGURE 7. The simulated average SAR (10 grams of tissue) distribution on human hand when the antenna is placed 5 mm above the wrist. The input power is fixed to 23 dBm. (a) Simulation model. (b) SAR profile of the reference antenna. (c) SAR profile of the proposed antenna. Their ground sizes are the same. (The εr value of the model material at 5.8 GHz is 27.5.)

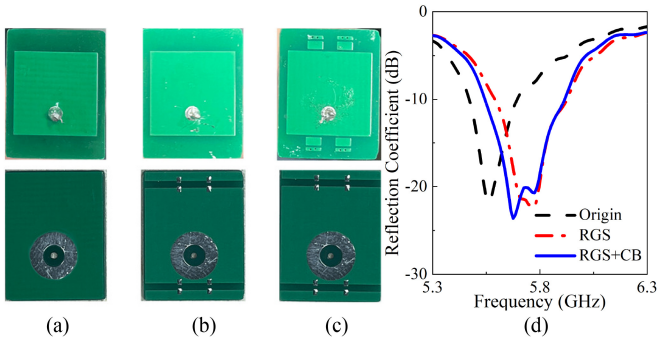

FIGURE 8. Fabricated prototypes. (a) Original patch antenna with finite ground. (b) RLGS loaded patch. (c) RLGS+CB loaded patch. (d) Measured reflection coefficients of the three antennas.

over a human wrist model in order to simulate the working condition of wearable devices. The average SAR (10 grams of tissue) distributions of the conventional patch antenna and the proposed one are also put together for comparison under the same ground size. It can be seen that the maximum average SAR of the reference antenna has reached 4.46 W/kg. In the meantime, the maximum average SAR of the proposed antenna sharply decreases to 0.22 W/kg. It means that the human body absorption from the radiator is negligible in this case, which makes the wearable device safer and the antenna performance steadier.

B. SIMULATION AND MEASUREMENT RESULTS

To verify the effectiveness of RLGS and CB loading, three prototypes of original patch, RLGS loaded patch, and RLGS+CB loaded patch are fabricated and measured. The photos of the models are shown in Fig. 8. The *S*-parameters and radiation performance of the fabricated prototypes are measured with Rohde & Schwarz ZVA vector network analyzer and SY-16M microwave chamber, respectively.

First of all, the measured results of the reflection coefficient of the prototypes are illustrated in Fig. 8(d). It can be learned that the loading of RLGS and CB has a mild influence on the resonance of the patch antenna, due to the extra current loop.

The simulated patterns of the prototypes are depicted in Fig. 9, which are normalized for the purpose of comparison.

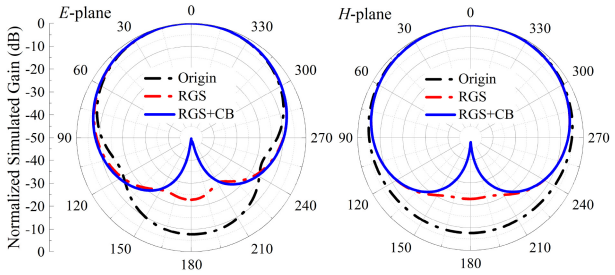

FIGURE 9. The self-normalized patterns of original patch, RLGS loaded patch, and RLGS+CB loaded patch in simulation (at resonance point).

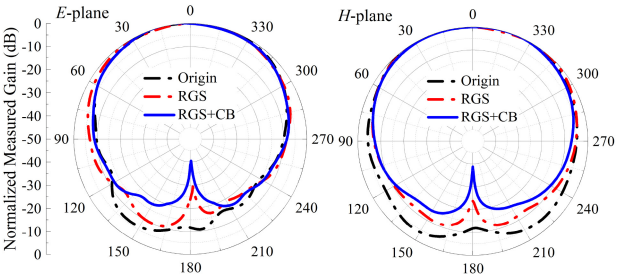

FIGURE 10. The self-normalized patterns of original patch, RLGS loaded patch, and RLGS+CB loaded patch in measurement (at resonance point).

The normalized reference is the maximum gain of each radiation patterns. Due to the limited ground design, the FBR of the original patch is as low as 7.65 dB. After merely loading RLGS to the patch, the FBR tentatively increases to 20.80 dB. It is not until the proposed RLGS+CB structure is loaded that the FBR is rapidly enhanced to 49.64 dB, which means that the backward radiation of the patch antenna with ultra-small ground has been removed.

The measured radiation patterns of the fabricated models are illustrated in Fig. 10, and a progressive relationship is also demonstrated. The measured FBR of the three prototypes are respectively 11.73, 22.27, and 38.68 dB. The effectiveness of RLGS and CB loading is identified through simulation and measurement. There are also certain differences between the simulated and measured results of radiation patterns and FBR. The reason is that the feeding cable of measurement equipment has a nonnegligible impact on the measured results. But, on the whole, the measured results are reasonable and satisfying.

Of course, the loaded resistance cuts down overall efficiency, which is recognized as a disadvantage when the antenna works in free space. However, when the antenna is applied in wearable condition, things will be very different. It is widely acknowledged that human body is highly lossy material and has a serious negative impact on the efficiency of wearable antennas. To demonstrate this effect, the antenna efficiency with and without a hand model are simulated and measured. As is shown in Fig. 11(b), the measured efficiency of the original patch antenna worn on hand is −4.25 dB at 5.8 GHz, which is 2.62 dB lower than the no-hand efficiency. In contrast, the measured efficiency of the

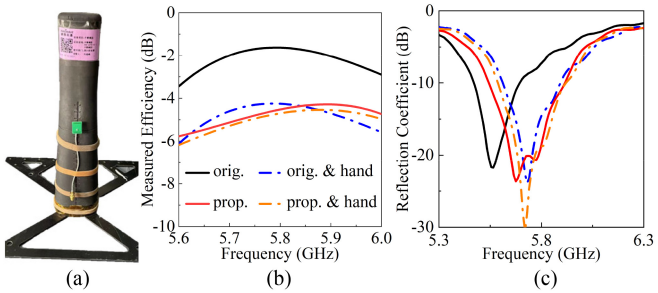

FIGURE 11. (a) Hand model used for measurement. The distance between the ground and hand is 5 mm. (b) Measured Total efficiency of the original patch and the proposed patch before and after being worn on a hand model. (c) Measured S11 of the antennas before and after being worn on a hand model. (The hand model type is SHO-GFPC-V1.)

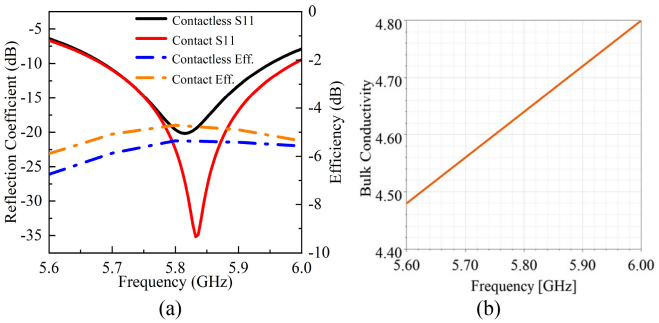

FIGURE 12. (a) The simulated performance of the proposed antenna before and after being fully contacted with human skin. The contactless situation is 5 mm over the hand model. (b) The conductivity of the hand model skin.

proposed patch worn on hand is −4.60 dB, which is only 0.18 dB lower than the no-hand efficiency. The efficiency changes above also indicate that the radiation power, which is supposed to be originally absorbed by human body, is now absorbed by the resistors instead.

Furthermore, the measured *S*-parameters are also illustrated in Fig. 11(c). The reflection coefficient of the proposed patch antenna remains steady after being worn on a hand model, while severe displacement occurs in the resonant frequency of the original patch. Clearly, the radiation parameters of the reference antenna are heavily dependent on the environment, which cannot ensure stable performance of wearable devices under different conditions. In contrast, performance of our proposed antenna is nearly unaffected by the human body and the SAR is extremely low. Even though the resistors absorb some power, the antenna efficiency under wearing condition is as good as the conventional patch antenna.

The performance of the proposed antenna when it is in contact with conductive surface such as human skin is also discussed. From Fig. 12. it can be seen that when compared with the reference contactless patch (5mm over the hand model), the efficiency of the contacted patch slightly drops. This phenomenon indicates that being contacted with skin only has little impact on antenna performance.

IV. CONCLUSION

In this article, a high-FBR patch antenna with a very small ground plane is proposed, and the equivalent circuit model of the introduced structure is established and analyzed. The back lobe suppression mechanism is perceived as a kind of far-field pattern superposition, in which the loaded ground slot is regarded as magnetic current. Through altering the RLGS and CB structure, the backward radiation from the ground slot and the original patch can be mutually cancelled out, so a high FBR can be achieved. The SAR of the proposed patch antenna can be enormously reduced as a consequence. The simulated and measured results demonstrate that the antenna can maintain particularly stable performance, and its *S*-parameters and total efficiency are nearly unaffected by the human body.

REFERENCES

[1] S. Maci, L. Borselli, and L. Rossi, "Diffraction at the edge of a truncated grounded dielectric slab," *IEEE Trans. Antennas Propag.*, vol. 44, no. 6, pp. 863–873, Jun. 1996.
[2] S. Maci, L. Borselli, and A. Cucurachi, "Diffraction from a truncated grounded dielectric slab: A comparative full-wave/physical-optics analysis," *IEEE Trans. Antennas Propag.*, vol. 48, no. 1, pp. 48–57, Jan. 2000.
[3] J. Huang, "The finite ground plane effect on the microstrip antenna radiation patterns," *IEEE Trans. Antennas Propag.*, vol. 31, no. 4, pp. 649–653, Jul. 1983.
[4] M. Sanad, "Microstrip antennas on very small ground planes for portable communication systems," in *IEEE Antennas Propag. Soc. Int. Symp. Dig.*, Jun. 1994, pp. 810–813.
[5] N. N. Gorobetz and N. P. Eliseyeva, "Optimizing radiation of microstrip and vibrator antennas by means of choosing form of the screen," in *Proc. Int. Conf. Antennas Propag.*, Apr. 1995, pp. 295–298.
[6] H. Zhang et al., "Design of low-SAR and high on-body efficiency tri-band smartwatch antenna utilizing the theory of characteristic modes of composite PEC-lossy dielectric structures," *IEEE Trans. Antennas Propag.*, vol. 71, no. 2 pp. 1913–1918, Feb. 2023.
[7] B. Pang, W. Hu, W. Jiang, and B. Lu, "Design of low-SAR terminal antenna using characteristic mode manipulation," *IEEE Antennas Wireless Propag. Lett.*, vol. 22, no. 4, pp. 749–753, Apr. 2023.
[8] H. H. Zhang et al., "Low-SAR MIMO antenna array design using characteristic modes for 5G mobile phones," *IEEE Trans. Antennas Propag.*, vol. 70, no. 4, pp. 3052–3057, Apr. 2022.
[9] S. Uda, "Wireless beam of short electric waves," *J. Inst. Electr. Eng. Jpn.*, vol. 49, no. 452, pp. 273–282, 1927.
[10] S. S. Jehangir and M. S. Sharawi, "A novel compact single layer semi-ring slot Yagi-like antenna with high front-to-back ratio," in *Proc. IEEE Asia–Pac. Conf. Antennas Propag. Conf.*, Jul. 2016, pp. 131–132.
[11] S. S. Jehangir and M. S. Sharawi, "A single layer semi-ring slot yagi-like MIMO antenna system with high front-to-back ratio," *IEEE Trans. Antennas Propag.*, vol. 65, no. 2, pp. 937–942, Feb. 2017.
[12] A. Elsherbini, J. Wu, and K. Sarabandi, "Dual polarized wideband directional coupled sectorial loop antennas for radar and mobile base-station applications," *IEEE Trans. Antennas Propag.*, vol. 63, no. 4, pp. 1505–1513, Apr. 2015.
[13] L. Zhang et al., "Single-feed ultra-wideband circularly polarized antenna with enhanced front-to-back ratio," *IEEE Trans. Antennas Propag.*, vol. 64, no. 1, pp. 355–360, Jan. 2016.
[14] K. Itoh, K. Konno, Q. Chen, and S. Inoue, "Design of compact multiband antenna for triple-band cellular base stations," *IEEE Antennas Wireless Propag. Lett.*, vol. 14, pp. 64–67, 2015.
[15] W. S. T. Rowe and R. B. Waterhouse, "Reduction of backward radiation for CPW fed aperture stacked patch antennas on small ground planes," *IEEE Trans. Antennas Propag.*, vol. 51, no. 6, pp. 1411–1413, Jun. 2003.

[16] T. Namiki, Y. Murayama, and K. Ito, "Improving radiation-pattern distortion of a patch antenna having a finite ground plane," *IEEE Trans. Antennas Propag.*, vol. 51, no. 3, pp. 478–482, Mar. 2003.
[17] Z. Liang, C. Lu, Y. Li, J. Liu, and Y. Long, "A broadband dual-polarized antenna with front-to-back ratio enhancement using semicylindrical sidewalls," *IEEE Trans. Antennas Propag.*, vol. 66, no. 7, pp. 3735–3740, Jul. 2018.
[18] G. H. Huff and J. T. Bernhard, "Improvements in the performance of microstrip antennas on finite ground planes through ground plane edge serrations," *IEEE Microw. Wireless Compon. Lett.*, vol. 12, no. 8, pp. 308–310, Aug. 2002.
[19] K. M. Luk and H. Wong, "A new wideband unidirectional antenna element," *Int. J. Microw. Opt. Technol.*, vol. 1, no. 1, pp. 35–44, Jun. 2006.
[20] L. Zhao et al., "Design of wideband dual-polarized ME dipole antenna with parasitic elements and improved feed structure," *IEEE Antennas Wireless Propag. Lett.*, vol. 22, no. 1, pp. 174–178, Jan. 2023.
[21] H. W. Lai, K. M. Mak, and K. M. Luk, "Cross slot antenna with very low back radiation for various wireless communications at 5.8GHz ISM band," in *Proc. IEEE MTT-S Int. Microw. Workshop Ser. RF Wireless Technol. Biomed. Healthc. Appl.*, Dec. 2013, pp. 1–3.
[22] C. Yang, Y. Yao, J. Yu, and X. Chen, "Novel compact circularly polarized antenna with high front-to-back ratio for UHF RFID reader applications," in *Proc. Asia Pac. Microw. Conf. (APMC)*, Dec. 2011, pp. 1358–1361.
[23] Y. Li, P. Yang, F. Yang, and S. He, "A method to reduce the back radiation of the folded PIFA antenna with finite ground," *Appl. Comput. Electromagn. Soc. J.*, vol. 28, no. 2, pp. 110–115, 2013.
[24] M.-C. Tang and R. W. Ziolkowski, "Efficient, high directivity, large front-to-back-ratio, electrically small, near-field-resonant-parasitic antenna," *IEEE Access*, vol. 1, pp. 16–28, 2013.